

EFFECT OF CONCRETE ENVIRONMENT ON THE CORROSION
PERFORMANCE OF EPOXY-COATED REINFORCING STEEL

A.A. Sagués
Department of Civil Engineering and Mechanics
University of South Florida
Tampa, Florida 33620

R.G. Powers
Materials Office
Florida Department of Transportation
Gainesville, Florida 32602

ABSTRACT

Corrosion of marine bridge substructure using concrete with epoxy-coated reinforcing steel has been observed in Florida Keys bridges. The mechanism of coating disbondment has been investigated by exposing regular production epoxy-coated rebars to liquid solutions of calcium hydroxide, sodium chloride, and calcium hydroxide with sodium chloride. Test exposures were conducted with freely corroding specimens and also under potentiostatic control with cathodic and anodic polarization. The calcium hydroxide-only solutions produced no adverse effects at any of the exposure conditions. The sodium chloride tests produced significant disbondment at the open circuit potential and under cathodic polarization. The mixed calcium hydroxide-sodium chloride solutions caused disbondment and corrosion under anodic polarization that reproduce much of the corrosion morphology observed in the field. It is tentatively proposed that corrosion in the field takes place at the anode of macrocells which result from the geometrical and environmental configuration of the substructure. The corrosion is aggravated by rebar fabrication and possibly by weathering of the rebar prior to construction.

Keywords: epoxy, coating, corrosion, disbondment, delamination, concrete, chloride, calcium hydroxide, bridges, macrocells, cathodic, polarization.

INTRODUCTION

Severe corrosion damage has been observed in the substructure of bridges in the Florida Keys^(1,2). This deterioration was unexpected since the reinforcing steel was epoxy-coated^(3,4,5) and the substructures affected were only six to nine years old at

Publication Right

the time corrosion was first observed. The damage, illustrated in Figure 1, affects approximately 1/3 of the bents in three major bridges in the area (Seven Mile Bridge, Long Key Bridge and the Niles Channel Bridge). The locations affected had an average of 2 inches (50 mm) of concrete cover over the rebar. Both fabricated and straight rebars show corrosion, typically in the region extending from 2 to 6 feet (0.6 to 1.8 m) above the high water line. Advanced stages of damage involve severe pitting (Figure 2), and accumulation of corrosion products between the epoxy and remaining metal as well as corrosion products in direct contact with the concrete. A chloride-rich liquid (pH typically 5.5) is observed frequently in freshly exposed rebar between the epoxy and the steel, even when the surrounding concrete was relatively dry (see Figure 3). Soundings under these conditions reveal extensive delamination of the concrete, which can be easily removed with a hammer. In the areas of severe corrosion, the coating was completely disbonded from the rest of the bar. Examination by a major epoxy powder supplier did not reveal any abnormal product characteristics.

In less severe cases of deterioration the coating could still be easily separated from the steel. The metal underneath appeared dull and slightly darkened. Disbondment of this type has been observed in portions of the substructure above the regions of greatest damage, as well as in the substructure of other south, central and west Florida bridges using epoxy coated rebar, with 7 to 11 years of service.

Disbondment of the epoxy coating is a likely precursor to the development of corrosion. Since corrosion was initially observed in fabricated rebar⁽¹⁾, the effects of bending on corrosion performance were investigated first. Recent research^(1,2) showed that bending epoxy-coated rebar to diameters used in common construction practice causes significant delamination of the coating, and that corrosion initiation is facilitated as a result. However, since severe damage has been observed also in straight bars, other mechanisms of corrosion initiation must have been present and need to be identified.

Factors that may initiate and propagate corrosion of straight coated rebar include weathering and damage produced by shipping and handling at the construction yard, the chemical environment of the rebar once in concrete, and galvanic coupling with other portions of the rebar or adjoining rebars. Electrochemical effects such as cathodic disbondment⁽⁶⁾ may be important under those circumstances. Some of these factors were addressed in this investigation by exposing epoxy-coated rebar specimens to various liquid chemistries. The test solutions chosen were 3.5% NaCl, saturated Ca(OH)₂, and saturated Ca(OH)₂ with 3.5% NaCl. These were intended as a first approach to investigate, respectively, the effects of weathering in a marine environment, behavior in uncontaminated concrete, and corrosion in chloride-containing concrete. In addition to freely corroding conditions, specimens were tested under potentiostatic control at potentials ranging from -1000 mV to +100 mV vs the Saturated Calomel Electrode (SCE). The exposures at the lower potentials were conducted to establish susceptibility to cathodic disbondment at potentials including those near the freely corroding values in chloride solutions (which are on the order of -650 mV vs SCE). Exposures at the higher potentials were aimed to investigate the situation where anodic portions of a bar are galvanically coupled to large cathodic regions elsewhere in the structure.

EXPERIMENTAL PROCEDURE

Epoxy coated rebar, size #10 (nominal diameter 1.25 inch (31 mm)) was obtained from a single heat of a regular production run by a major supplier of the Florida Department of Transportation (FDOT). The material adhered to the current FDOT specifications (based on AASHTO designation M284-66 / D3963-82). The fusion-bonded

epoxy coating material was a bisphenol-amine product widely used for reinforcing steel coating in the U.S. The coating had a typical thickness of 0.15 mm. Surface condition was rated A, which is the highest score in the 5-point rating scale used by the FDOT. This corresponds to absence of surface damage detectable by naked-eye observation.

The bar was cut into 30 cm long specimens. The ends of each specimen were covered with epoxy field-patching compound. One of the ends was cast in a short cylindrical plug of epoxy metallographic mounting compound. The other end was drilled and tapped for electrical connection. The specimens were exposed to the test solutions either in the as-received surface condition or after intentional surface damage. The latter consisted of exposing small amounts of bare metal by means of a sharp file. Five markings nominally 1 mm wide, 4 mm long were introduced at regular intervals on one side of the specimen by filing on the top of deformation ribs. Five additional markings, 1 mm by 6 mm, were introduced on the other side (see Figure 4). All markings were in the portion of the bar which was in contact with the test liquid. The amount of metal intentionally exposed was approximately 0.25 % of the total area of specimen in contact with the liquid.

Three types of water-based test solutions were used, as detailed in Table I. The tests were conducted in rectangular tanks with 40 liters of solution, in which the specimens were submerged vertically (see Figure 4). For each test solution, pairs of specimens in up to four different polarization conditions were tested together. The nominal exposure duration was 30 days. Fresh solution was used at the beginning of each test. Additionally, in one of the tests (Solution II, specimens with intentional surface damage) the liquid was renewed weekly. The solution temperature was 21 (± 1)°C.

Specimens were polarized at preselected potentials by means of individual potentiostatic control circuits. All circuits in each tank shared a common stainless steel strip counter electrode, which ran flat across the lower perimeter of the tank. To avoid problems such as electrode tip clogging, an activated titanium reference electrode was used as a master reference for all the circuits in any given tank. Potential settings and periodic minor adjustments were made using an SCE momentarily in contact with the test solutions. The arrangement provided reliable operation throughout the test sequence.

The electrical current demand of potentiostated specimens and the open circuit potential of freely corroding specimens were monitored during the test period. Electrochemical impedance spectroscopy (EIS) measurements of selected specimens exposed to open circuit conditions were obtained in a separate test cell with the same liquid chemistry as in the test tank. The counter electrode consisted of twin graphite rods placed along the full length on each side of the specimen. The reference electrode was placed 6 mm apart from the middle of the specimen front.

At the end of the exposure the specimens were removed from the test solution, lightly rinsed with distilled water and blot-dried with a paper towel. A sharp knife was used to remove the coating from areas where disbondment had occurred. A pH micro-electrode was used to measure the pH of liquid that was present at some corroded or disbonded regions. Disbonded or damaged areas were measured by tracing on a transparent plastic sheet rolled on the specimen, and later placing the unrolled sheet on graph paper.

RESULTS

A summary of the tests conducted and their exposure parameters is given in Table II. Highlights of results for each test environment are given below. All electrode potentials in the following text are versus SCE. The amount of disbondment observed in each case, expressed as a fraction of the area of bar in contact with the liquid, is presented graphically in Figure 5. Integrated current demand for potentiostated specimens is presented in Figure 6.

Solution Type I, Saturated Calcium Hydroxide.

Exposure to this environment at all test conditions caused no visible corrosion and virtually no disbondment. The appearance of the coating was essentially the same in both the submerged and above-water portions of the test specimens. The exposed metal in the intentionally damaged portions was bright. The potential of the open circuit specimens was in the passive region. Limited EIS testing conducted on the material exposed to open circuit conditions revealed that the magnitude of the electrochemical impedance at low frequency (~ 0.001 Hz) was in the megohm range for both as-received and intentionally damaged specimens. Additional characterization of the high-frequency impedance response is in progress.

Solution Type II, Sodium Chloride.

Specimens exposed at -1000 mV in the as-received condition and at -750 mV with surface distress showed significant disbondment. In the as-received material the coating could be easily lifted around minute surface imperfections, usually located at the outer region of deformation ribs. These imperfections appeared to be the result of contact between bars during shipping or during handling. The disbonded regions were roughly circular around the imperfections, with radii as large as 10 mm. The metal underneath was bright with no visible deposits or corrosion products. The material with surface distress showed essentially the same resulting morphology, extending mainly from the intentionally damaged regions.

Under open circuit conditions, both the specimens with as-received and those with intentionally damaged surfaces developed about the same average corrosion potentials (~ -645 mV). In the as-received material orange rust spots appeared at minor surface imperfections. The coating was disbonded typically for a distance of 3 mm around these imperfections. In the intentionally damaged specimens orange corrosion products developed on about two-thirds of the exposed metal spots, while the rest remained bright through the test. However, disbondment was observed around both the bright and rusty exposed metal to a typical distance of 3mm. The metal underneath the disbonded coating in all cases remained bright. No conspicuous accumulation of liquid was observed between the coating and the metal. The EIS behavior of the as-received specimens after about one month of exposure is exemplified in Figure 7. Also shown are the impedance spectra of a specimen with intentionally damaged surface early in and near the end of the one month test.

At -500 mV corrosion product crests were conspicuous at minor imperfections in the as-received material and at the exposed metal on the intentionally distressed specimens. There was considerable metal loss underneath the corrosion product crests. The loss was in the form of corrosion pits. These resembled short drilled craters in the as-received material, and were broader or elliptical in the intentionally distressed material, following the shape of the initial damage. No coating disbondment could be discerned immediately surrounding the perimeter of the pits. The pits were filled with a dark, pasty corrosion product. Some liquid was present at the pits and some of the disbonded areas, but in too small an amount to characterize.

Only the as-received specimens were tested in this environment at a higher potential (+100 mV). Large orange corrosion product accumulations developed at minor surface imperfections. Significant metal loss, in the form of sharp, circular craters was present below. The pits were filled with dark, powdery corrosion products and no free liquid. As in the -500 mV tests, no significant coating disbondment was observed around the pits.

Solution Type III, Sodium Chloride with Calcium Hydroxide.

The specimens with and without intentional surface damage, exposed to -750 mV and -1000 mV respectively showed no corrosion products. Virtually no disbondment was observed in the as-received material; a small amount of disbondment took place at the intentionally damaged specimens. There was no fluid accumulation at crevices and all the metal surfaces examined were bright.

Open circuit potentials for both the as-received and the intentionally distressed specimens were close to -625 mV. The as-received material showed no external corrosion products, but a few small blisters were observed at minor surface imperfections, near the top of deformation ribs where mechanical contact with hard surfaces may have occurred earlier. There was disbondment, about 1mm around the center of those blisters. The metal underneath was bright. The specimens with filed spots showed a minor amount of corrosion products on about one-third of those spots; the remainder showed bright metal. Disbondment was observed for about 1 mm around all the filed spots, regardless of whether corrosion products were present or not. The metal underneath the disbonded coating was bright. The EIS behavior in this environment is still under characterization.

Specimens exposed at -500 mV showed external corrosion products in the form of red-black crests growing outside coating imperfections (either preexisting or intentionally made, but much more conspicuous in the latter case). Only about three quarters of the intentionally damaged regions showed corrosion; the exposed metal remained bright on the rest. There was significant disbondment of the coating at the imperfections (typically 3 mm around). The metal underneath was usually dark near the initial opening and bright further in. The disbonded regions contained a clear liquid with a pH between 4 and 5. At the corroded zones some visible metal dissolution had taken place in the form of small pits, typically a fraction of a mm deep.

At -400 mV (intentionally damaged coating only tested) conspicuous external corrosion products were seen at all the damaged spots and also at some preexisting, small holidays. The corrosion crests resembled red and black tubercles. Underneath the coating imperfection circular corrosion pits, as large as 6 mm in diameter were present (see Figure 8). The pits were filled with pasty, black corrosion products. Around the pits and at the smaller imperfections disbondment took place to a distance of 3 to 10 mm. The underlying metal was dark near the imperfection and bright further away. Clear liquid with a pH between 4 and 5 was present in the disbonded region and liquid-filled blisters had formed at places.

The only specimens exposed at +100 mV were in the as-received surface condition. The corrosion morphology closely resembled that described in the previous paragraph, but the number of corroded regions, pit size and extent of disbondment was smaller.

DISCUSSION

Cathodically Polarized Specimens

The results showed that Solution Type II (3.5% NaCl) produced disbondment mainly under cathodic polarization, while Solution Type III (sodium chloride plus calcium hydroxide) caused conspicuous delamination only at anodic potentials. The calcium hydroxide-only Solution Type I did not cause observable delamination in any of the test conditions.

The disbondment observed in the tests with Solution Type II had the typical characteristics observed in cathodic disbondment phenomena^(6,7,8,9). Cathodic disbondment is generally thought to result from the alkalinity generated at the cathodic site by reactions such as oxygen reduction. The hydroxyl ions may affect the integrity of the polymer coating where it joins the metal, by saponification or other adverse interactions^(10,11), thus permitting the separation from the substrate. Another possible mechanism is the reduction at the surface of the steel of the oxides to which the coating is adhered^(6,8,12). Epoxies such as the coating used here tend to be highly resistant to alkaline deterioration^(13,14), so the latter mechanism appears to be more likely. Cathodic disbondment necessitates the presence of a suitable cation at the coating-metal interface to maintain charge balance^(6,15). Alkaline metal ions such as Na, present in solution Type I, fulfill that role in chloride solutions^(6,16). At present there is not enough information on the proprietary coating used in this application to indicate whether ionic transport to the disbondment front takes place laterally or through the coating.

Cathodic disbondment is not promoted by calcium ions^(6,16,17,18); this is consistent with the absence of delamination in Solution Type I (calcium hydroxide only) since currents were cathodic (or of very small magnitude) over the entire potential range tested. The absence of extensive disbondment at low potentials in Solution Type III cannot be easily explained since the same amount of sodium and chloride was present there as in Type II Solution. The calcium ions appear then to have played an active role in reducing disbondment at low potentials. In the hardened concrete environment the situation may be different because the pore water solution appears to be richer in sodium and potassium ions, and lower in calcium ions^(19,20), than the Solution Type III used in the present experiments.

Freely Corroding Conditions

The exposed steel surface in Solution Type I was passive in the entire range of potentials tested, so that no corrosion product accumulation was observed. This was consistent under open circuit potential conditions by the large magnitude of the electrochemical impedance observed.

The specimens exposed to Solution Type II under open circuit conditions showed corrosion products only at some of the exposed metal spots. This indicated that some of the spots were acting as macrocathodes while anodic reactions were concentrated on those spots showing corrosion product accumulation. Because of the high electrolyte conductivity the potential drop between macroelectrodes is not expected to have been excessive. This is in agreement with the observation that the degree of disbondment was about the same in all intentional damage areas whether corrosion products were present or not. The electrochemical impedance behavior was largely as expected from similar systems⁽²¹⁾. All specimens showed depressed semicircular impedance diagrams. These can be interpreted as resulting from the coupling of the impedance of an activation-limited metal dissolution process with that of a cathodic reaction (oxygen reduction). The high-frequency limit of the impedance, which is indicative of the effective solution resistance was an order of magnitude higher for the as-received

material than for the specimens with intentional surface damage. That agrees well with the virtually unblemished appearance of the as received material, compared with the presence of about $1/3 \text{ cm}^2$ of bare metal in the specimens with surface distress. The same applies to the low frequency limit of the impedance magnitude, where the distressed material shows a considerably lower value. The apparent polarization resistance in Figure 7 B near the end of the one-month exposure was $\sim 1 \text{ kohm}$. Using a typical conversion constant value $B=26 \text{ mV}^{(21,22)}$ this corresponds to a corrosion current of 26 uA . The nominal, averaged corrosion current density, based on the initial amount of bare metal in contact with the liquid, was then on the order of 80 uA/cm^2 . That value approaches the typical limiting current density for oxygen reduction at an extended flat electrode in still, naturally aerated water⁽²³⁾. This is only an order-of-magnitude comparison, since the system geometry here is complicated, there is significant frequency dispersion, and the measurements showed that the apparent polarization resistance decreased with increasing exposure time. The change in impedance behavior with time may have resulted from additional cathodic surface being made available by disbondment, or from the accumulation of electronically conductive corrosion products in contact with the metal surface⁽²¹⁾. Those two phenomena could account, separately or together, for the frequency dispersion manifested in the appearance of depressed semicircles^(21,24). Keeping in mind the limited amount of available data, the results nevertheless suggest that oxygen reduction at the areas of coating damage can account for the estimated rates of corrosion. Thus, oxygen diffusion through the coating was not necessarily a major contributor to the cathodic reaction in this particular case.

The admittances of the Faradaic processes and interfacial capacitances present were relatively high, even for the specimens in the as-received condition. Assuming a typical coating thickness of 0.15 mm , and a dielectric constant of about 3, the coating capacitance in the specimens used is on the order of 1 nF . The corresponding impedance magnitude at 10 KHz is over 10 Kohm , while the impedance measured at that frequency was always at least an order of magnitude lower. Because of that, the presently available high frequency data cannot be used to study the evolution of the coating capacitance as a function of exposure time in the specimens exposed in Solution Type II.

Anodic Behavior

The anodically polarized specimens in Solution Type II showed considerable pitting but little or no delamination adjacent to the pits. This is in agreement with the behavior observed in other systems where anodic exposure to NaCl solutions was investigated^(6,7,8,18).

The anodic behavior in Solution Type III is of interest because both extensive pitting and delamination took place, and the corrosion morphology strikingly resembled that observed in the field. The accumulation at the pits and blisters of liquid with pH between 4 and 5, when the pH of the bulk solution was 12.5, had to be the result from an efficient process of local acidification. A likely mechanism is the hydrolysis of ferrous ions, which are created by the iron dissolution reaction at the local anode. This process in chloride solutions can generate local pH values in the 4-5 range as observed in occluded cells^(9,23,25). The specimens examined here showed darkening, indicative of local metal dissolution, underneath the disbonded coating next to the pits or at blistered areas.

The corrosion morphology in the anodically polarized specimens in Solution Type III may then be interpreted by the following tentative mechanism: Metal loss, driven by the externally impressed current, is assumed to begin first at a coating damage

spot. Corrosion continues there, sometimes forming a pit. Because of the presence of the calcium hydroxide, corrosion at the initial point may become arrested or proceed more slowly than in the sodium chloride-only solutions. Anodic action extends however into the tighter edge surrounding the spot. There the accumulation of ferrous ions promotes more efficiently both the buildup of chloride ions and acidification by hydrolysis⁽²³⁾. These conditions initiate a self-propagating crevice between the coating and the metal. The process continues with the zone at the edge of the crevice being always the more active while the thickening trailing gap is influenced by the partially passivating bulk electrolyte chemistry. The disbondment would then be the result of metal dissolution underneath the coating (anodic undercutting⁽⁶⁾).

The mechanism proposed above is consistent with the observation that at -500 mV, anodic currents in the NaCl solution were over an order of magnitude greater than in the NaCl-Ca(OH)₂ solution (see Figure 6). Other matters require explanation, such as the presence of the zone of bright metal disbondment observed sometimes ahead of the dark metal crevice. Conditions in that zone can be complicated by the many factors present in an occluded cell; for example, the potential deep into the crevice may differ by several hundred mV from that at the opening^(25,26,27). The transport of solution species through the coating may be another important consideration, but as indicated earlier, there is not enough information available on this item. The chloride permeability of some coatings of this type has been reported to be unmeasurably low^(28,4). On the other hand, the coating material used here does absorb water, and its transport to regions where chloride may have accumulated below the coating can be expected to take place^(7,15).

Service Conditions

The results showed that significant disbondment can be caused by exposure to conditions addressing weathering and service in chloride-containing concrete. The tests in the sodium chloride solution showed that a sizable fraction of the coating can lose adherence under open-circuit conditions. This result merits attention when considering that rebar bundles are frequently subject to weathering at shoreside storage yards for extended periods (months) while subject to various degrees of seawater spray. The steep dependence of the extent of disbondment with potential (Figure 5) suggests that macrocell action (not unlikely in bundles with trapped moisture) could severely aggravate local disbondment. Fabrication of the rebar is expected to strongly increase the likelihood of deterioration⁽²⁾.

Once in place, reinforced concrete marine substructure columns develop moisture and chloride accumulation patterns that can create very active corrosion macrocells^(29,30). The high environmental humidity and temperature existing in southern Florida promote low concrete resistivity which in turn permits macroscopic interaction distances. The long, vertical bars commonly used in substructure columns provide lengthwise electronic conductivity. Chance contact at tie wires or overlapping semiconductive corrosion products may bring other portions of the structure into the galvanic circuit as well. The intensity of the macrocell will be expected to be greater if the effective cathode area has been increased by previous damage, including fabrication and weathering as discussed above.

The behavior observed in the anodically polarized specimens in Solution Type III reproduces most features of the damage observed in the above-tide area. This suggests that the corrosion seen in the affected structures may take place at the anodic end of extended macrocells. If that is the case, the results of this investigation suggest that the presence and distribution of coating imperfections can be a critical factor in deciding the long term performance of the material. Currently used acceptable

damage criteria (for example 2% of metal exposed, up to 1/4 inch (6mm) long defects, etc.⁽³¹⁾) may be too permissive. Likewise, patching methods for damaged bar using liquid curing epoxy may not guarantee enough protection because of the higher permeability of the patching material⁽⁴⁾. The distribution of the damage may be equally important. Because the extent of anodic polarization increases as a function of cathode to anode area ratio, it is quite possible that selecting the rebar with the best surface condition for the zone of most severe corrosion in a column may result in dangerously localized pitting.

The investigation presented here represents an initial effort to understand the causes of an unexpected materials performance problem. Additional tests and observations are in progress to obtain a more accurate view of the mechanisms involved. Nevertheless, the experience in the field and the laboratory experiments performed to date suggest that particular attention and care may be needed for successful, long term performance of epoxy-coated rebar in aggressive substructure service. Requirements may include extremely low holiday frequency, and shipping, handling and fabrication procedures significantly improving over current practice. Strict weathering protection, the specification of maximum rebar element dimensions, and possibly verifiable isolation between individual rebar segments may require implementation.

CONCLUSIONS

1. The adherence of the coating remained unaffected by exposure to the saturated calcium hydroxide solution over the exposure time and potential range tested.
2. Delamination with the characteristics of cathodic disbondment was observed after exposure to 3.5 % sodium chloride solution at the freely corroding and lower potentials. Exposure under anodic polarization resulted in pitting but little disbondment.
3. Exposure to the mixed calcium hydroxide-sodium chloride environment did not result in extensive disbondment at cathodic potentials. However, exposure under anodic polarization resulted in both pitting and delamination. The corrosion morphology of the anodically polarized specimens resembled the damage observed in the field.
4. The deterioration observed in the field can be interpreted as resulting from the combination of several adverse factors. These include a severe weathering environment prior to construction, damage due to handling and fabrication, and the propensity for development of corrosion macrocells at the substructure in subtropical marine applications.

ACKNOWLEDGMENT

This work was supported by the Materials Office, Florida Department of Transportation, in cooperation with the U.S. Department of Transportation. The opinions, findings and conclusions expressed here are those of the authors and not necessarily those of the supporting agencies.

REFERENCES

1. R. Kessler and R. Powers, Interim Report "Corrosion Evaluation of Substructure, Long Key Bridge", Corrosion Report No. 87-9A, Materials Office, Florida Department of Transportation, Gainesville, Florida, 1987.

2. A.Zayed, A.Sagues and R.Powers, "Corrosion of Epoxy-Coated Reinforcing Steel", Paper No. 379, Corrosion/89, National Association of Corrosion Engineers, Houston, 1989.
3. D.Gustafson, Civil Engineering Vol.58, p.38, October 1988.
4. L.Salparanta, "Epoxy Coated Concrete Reinforcements". Research Report 525 (ISBN 951-38-3094-2), Technical Centre of Finland, Espoo, March 1988.
5. Y.Virmani, K.Clear and T.Pasko, "Time to Corrosion of Reinforcing Steel in Concrete Slabs", Vol.5: Calcium Nitrite Admixture and Epoxy-Coated Reinforcing Bars as Corrosion Protection Systems, Report No.FHWA/RD-83/012, National Technical Information Service, Virginia, 1983.
6. H.Leidheiser, "Coatings" in Corrosion Mechanisms, p.165, F.Mansfeld, Ed., 1987.
7. H.Leidheiser, "Mechanisms of De-adhesion of Organic Coatings from Metal Surfaces", in Polymeric Materials for Corrosion Control, ACS Symp. Series 322, p.124, R.Dickie and F.Floyd, Eds., American Chemical Society, Washington, 1986.
8. E.Koehler, "Corrosion Under Organic Coatings", in Localized Corrosion, NACE-3, p.117, R. Staehle et al, Eds., National Association of Corrosion Engineers, Houston, 1974.
9. H.Leidheiser and M.Kendig, Corrosion, Vol.32, p.69, 1976.
10. R.Dickie and T.Smith, Chemtech, p.31, January 1980.
11. J.Hammond, J.Holubka, J.DeVries and R.Dickie, Corrosion Sci., Vol.21, P.239, 1981.
12. J.Thornton, J.Cartier and R.Thomas, in Polymeric Materials for Corrosion Control, ACS Symp. Series 322, p.169, R.Dickie and F.Floyd, Eds., American Chemical Society, Washington, 1986.
13. R.Dickie, in Polymeric Materials for Corrosion Control, ACS Symp. Series 322, p.136, R.Dickie and F.Floyd, Eds., American Chemical Society, Washington, 1986.
14. H.Hodo, T.Tsuda, K.Ogasawara and T.Takizawa, in Polymeric Materials for Corrosion Control, ACS Symp. Series 322, p.314, R.Dickie and F.Floyd, Eds., American Chemical Society, Washington, 1986.
15. G.Walter, Corrosion Sci., Vol 26, p.27, 1986.
16. K. McLeod, "Blistering of Paint Films", D.Phil Thesis, Oxford, 1984.
17. J.Sykes and K.McLeod, "Cathodic Blistering of Marine Coatings in Salt Solutions", Corrosion Research Symposium, Extended Abstracts, p.46, Corrosion/84, National Association of Corrosion Engineers, Houston, 1984.
18. W.Schwenk, "Adhesion Loss of Organic Coatings; Causes and Consequences for Corrosion Protection" in Corrosion Control by Organic Coatings, p.103, H.Leidheiser, Ed., Nat. Association of Corrosion Engineers, Houston, 1981.

19. K.Anderson, B.Allard, M.Bengtsson and B.Magnusson, Cement and Concrete Research, Vol.19, p.327, 1989.
20. A.Moragues, A.Macias and C.Andrade, Cement and Concrete Research, Vol.17, p.173, 1987.
21. A.Zayed and A.Sagues, in press (Corrosion Sci.).
22. F.Mansfeld, "The Polarization Resistance Technique", in Advances in Corrosion Science and Technology, Vol. 6, M.Fontana and R.Staehle, Eds., Plenum Press, New York, 1976.
23. M.Fontana, Corrosion Engineering, 3rd. Edition, McGraw-Hill, New York, 1986.
24. A.Sagues, "Evaluation of Corrosion Rate by Electrochemical Impedance in a System with Multiple Polarization Effects", Paper No.25, Corrosion/89, National Association of Corrosion Engineers, Houston, 1989.
25. A.Turnbull, Corrosion Sci., Vol. 23, P.833, 1983.
26. R.Parkins, I.Craig and J.Congleton, Corrosion Sci., Vol.24, P. 709, 1984.
27. H.Pickering, Corrosion, Vol.42, p.125, 1986.
28. R.Pike, R.Hay, J.Clifton, H.Beeghly and R.Mathey, Public Roads, Vol.37, p.185, 1973.
29. A.Aguilar, A.Sagues and R.Powers, "Corrosion Measurements of Reinforcing Steel in Partially Submerged Concrete Slabs", in Corrosion Rates of Steel in Concrete, N.Berke, Ed., STP 1065, ASTM, Philadelphia, 1990.
30. M.Makita, Y.Mori and K.Katawaki, "Marine Corrosion Behavior of Reinforced Concrete Exposed at Tokyo Bay", in ACI Publication SP-65, Performance of Concrete in Marine Environments, p. 271, V.Malhotra, Ed., American Concrete Institute, Detroit, 1980.
31. Guidelines for Inspection and Acceptance of Epoxy-Coated Reinforcing Bars at the Job Site, 1st. Ed., Concrete Reinforcing Steel Institute, Schaumburg, Illinois, 1986.

Table I

Liquid Test Solutions

Type I Water with 10 g/l Ca(OH)_2 added ^{a,b} (pH~12.5)

Type II Water with 3.5% NaCl ^a (neutral pH)

Type III Water with 3.5% NaCl and 10 g/l Ca(OH)_2 added ^{a,b} (pH~12.5)

Notes:

a: The water was tap water purified by reverse osmosis to obtain a typical resistivity of 20,000 ohm-cm.

b: Undissolved Ca(OH)_2 was allowed to precipitate to the bottom of the test tank.

Table II

Experimental Conditions

The table indicates with an X the Solution Type and electrode potential (vs. SCE) combinations tested, for specimens in the as-received condition and for specimens with intentional surface damage. O.C. represents open circuit tests.

Solution Type	As-Received				Intentionally Damaged			
	Potential (mV)				Potential (mV)			
	-1000	O.C.	-500	+100	-750	O.C.	-500	-400
I	X	X ^a	X	X	X	X ^b	X	X
II	X	X ^c	X	X	X	X ^d	X	---
III	X	X ^e	X	X	X	X ^f	X	X

Note: Open circuit potentials were measured throughout the test duration. The average values for each test condition were as follows:

- a: -158 mV b: -131 mV
- c: -645 mV d: -643 mV
- e: -607 mV f: -615 mV



FIGURE 1 - General appearance of corrosion in a bridge column using epoxy-coated reinforcing steel.



FIGURE 2 - Appearance of a #5 reinforcing bar (horizontal hoop portion of a bridge substructure column) after sandblasting.



FIGURE 3 - Left: Knife incision on a corroding vertical #8 rebar just after removing the concrete cover, showing liquid flowing out of the cut; the surrounding concrete was not wet. Right: The same area after separating the coating.

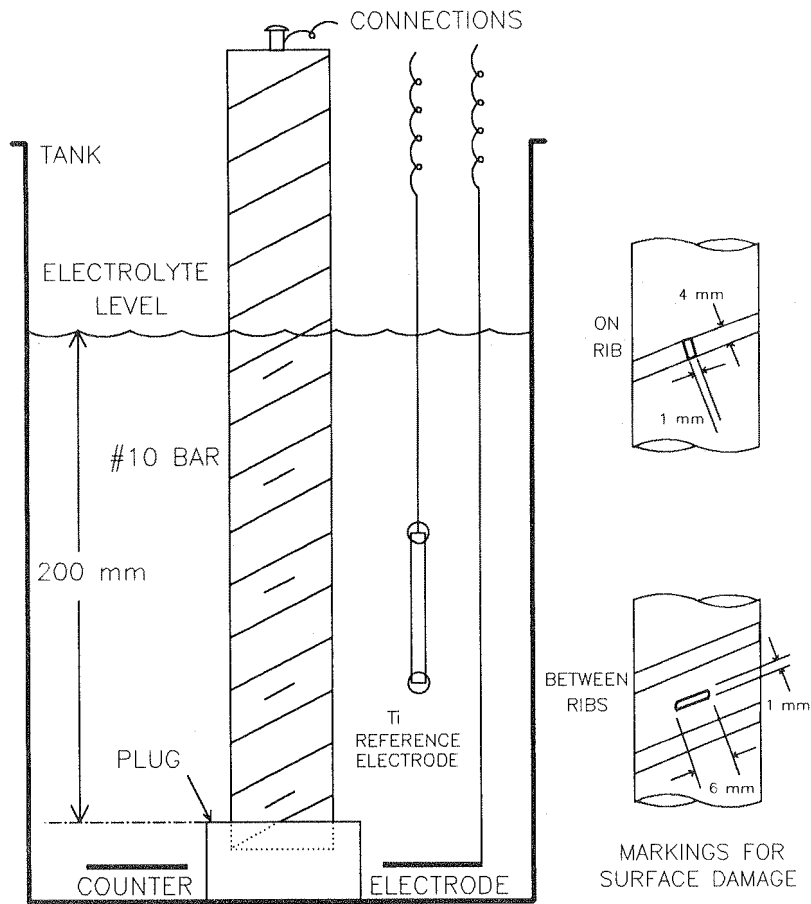


FIGURE 4 - Specimen and electrode setup for the potentiostatic exposures.

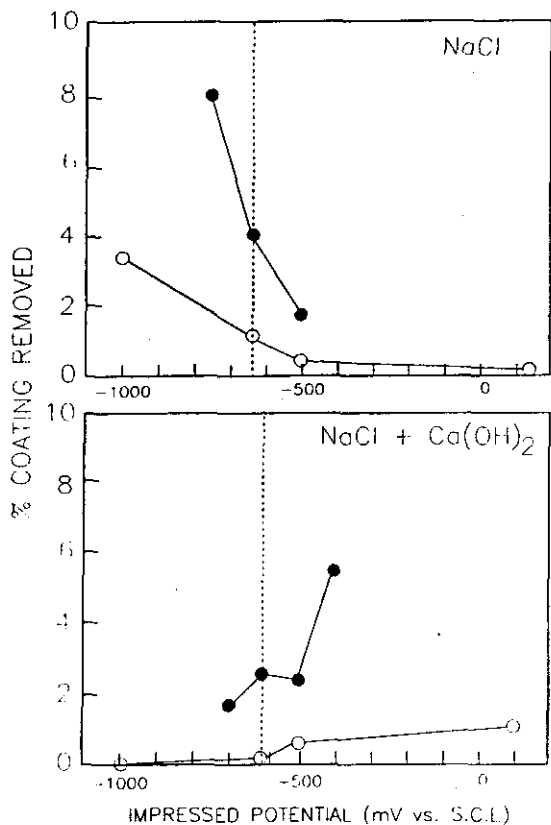


FIGURE 5 - Average percentage of coating that could be removed by sliding a knife between the coating and substrate after the one-month exposure to the chloride-containing environments. The results are given as a function of the impressed potential (open circuit condition shown by dashed line). Open symbols (○): as-received material. Closed symbols (●): intentional surface damage. The calcium hydroxide-only solution resulted in negligible disbondment.

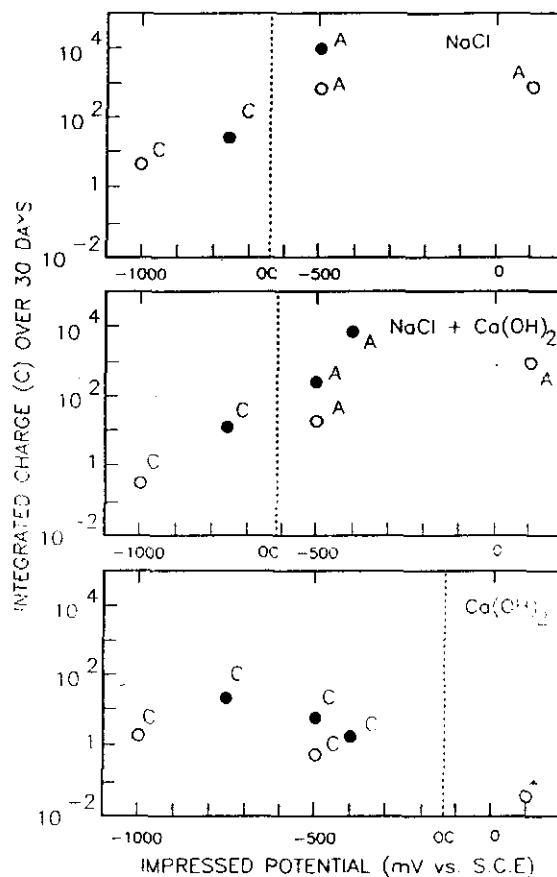


FIGURE 6 - Integrated electric charge (one month nominal exposure time) as a function of impressed potential for the three environments tested. The results are the average from duplicate specimens. The open circuit condition is shown by the dashed line. Open symbols (○) designate as-received material; closed symbols (●) designate intentional surface damage. A and C correspond to anodic and cathodic currents respectively. The current in the +100 mV tests in the calcium hydroxide environment (*) was small and its polarity fluctuated; the average was cathodic.

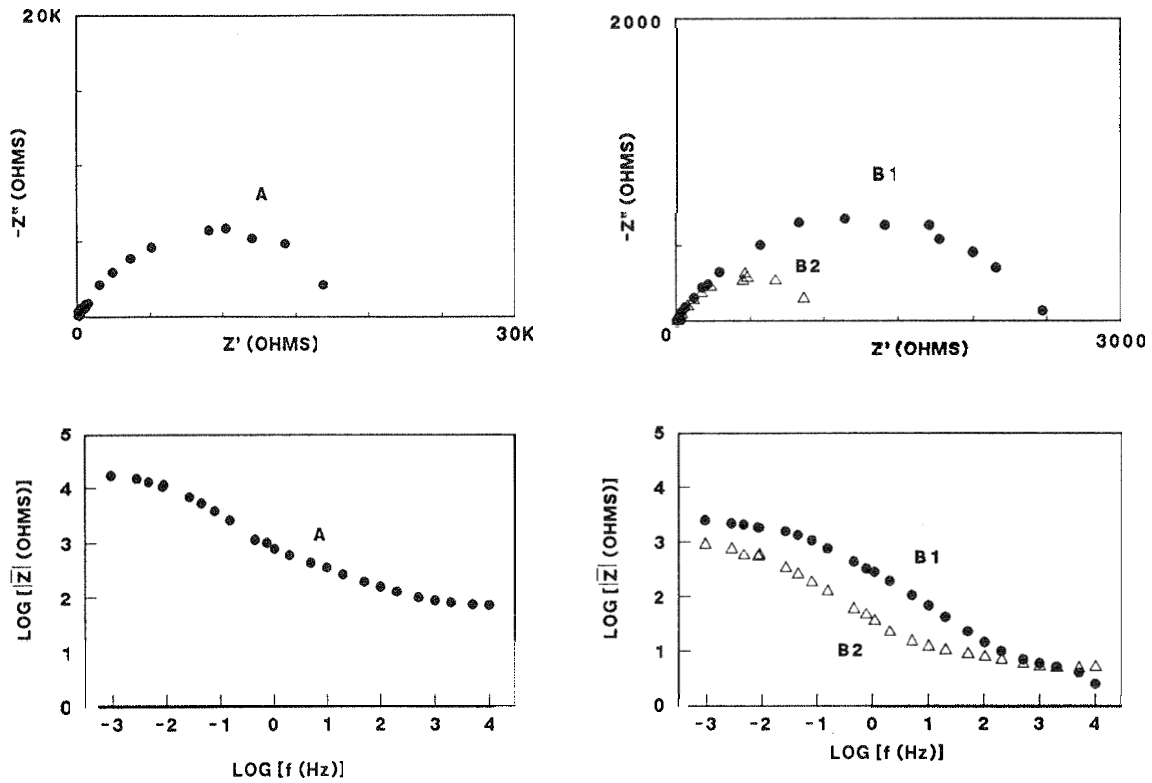


FIGURE 7 - EIS behavior of specimens in the sodium chloride solution (Type II).
 A) Material in the as-received condition, one month of exposure.
 B) Material with intentional surface damage; B1:one week; B2:one month of exposure.

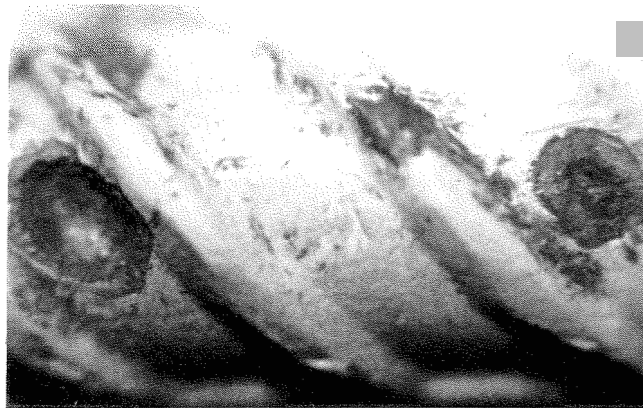


FIGURE 8 - Appearance of the surface after removing disbonded coating from a specimen exposed to Solution Type III (calcium hydroxide plus sodium chloride) for one month at -400 mV vs SCE.